

VASCULAR NETWORK TRACKING IN SLO OCULAR FUNDUS IMAGES FOR STATIC AND DYNAMIC PARAMETER EXTRACTION

Tomaso Bufalini, Ada Fort, Leonardo Masotti, Riccardo Pini

Dept. of electronic Engineering - University of Florence - Via S. Marta 3 - 50139 Florence - Italy

ABSTRACT

In this work a tracking algorithm which extracts the vascular network structure from *fundus* Scanning Laser Ophthalmoscope (SLO) images is presented. The tracking algorithm is based on *a priori* knowledge of the vessel structure. It exploits the continuity of radius, position, direction and brightness of a blood vessel and is based on a recursive strategy. First, a main vessel is tracked and its branch points on both sides are identified. Then, the tracking process is applied again to the identified branches. The procedure is repeated till no branch points are found. The output of the algorithm is a structural description of the vascular network consisting of vessel position, radius and curvature. The presented algorithm was developed for images obtained using a contrast agent (fluoroangiography) but was also adapted to images without any contrast agent. The algorithm was tested both on simulated and real images and proved to give accurate measurement of vessel radius and position (mean errors below 1 pixel).

1 INTRODUCTION

Fundus analysis is very important for an early diagnosis of some common diseases. In particular hypertension can be detected at early stages by the analysis of fundus vessel network [1]. In fact it was proved that this disease modifies the retinal vascular network changing some of its static and dynamic parameters, such as vessel diameter, vessel curvature, bifurcation angles and pulsatility.

The evaluation of these parameters, obtained by monitoring the *fundus*, can be of the utmost clinical relevance if measurement repeatability is achieved. This can be obtained by using an automated technique [2], [3].

To this purpose a tracking algorithm was developed to extract the vascular network structure from fundus images obtained by SLO, an optical instrument which provides images with high contrast and high resolution [4]. The algorithm is based on *a priori* knowledge of the vessel structure; it exploits continuity of radius, position and direction of each vessel. The algorithm gives a structural description of the vessel network in terms of vessel centerline position, vessel radius and vessel direction. Thus, the extraction of the relevant parameters for the whole network is straightforward. The network extraction process is based on a recursive strategy. The tracking of a main vessel is performed and its branch points are found; the tracking is repeated for the identified branches. The extraction ends when no more branch points are detected.

2 ALGORITHM DESCRIPTION

The tracking process is started by the physician, who gives the initial position \mathbf{P}_0 of the vessel centerline, the initial direction \mathbf{u}_0 and the initial radius R_0 .

The k -th step of the tracking process can be described as follows (see Figure 1). Given the current centerline point, \mathbf{P}_k , the current direction, \mathbf{u}_k , and the current radius, R_k , the point \mathbf{P}'_{k+d} , which is the point located at a distance d from \mathbf{P}_k along \mathbf{u}_k , is determined. The distance d , according to the continuity principles, is proportional to R_k . The point \mathbf{P}'_{k+d} is the first approximation of the new centerline point (\mathbf{P}_{k+d}). The brightness $B(x,y)$ is sampled on a segment perpendicular to the direction \mathbf{u}_k and centred on \mathbf{P}'_{k+d} , so the brightness profile $b_k(i)$ is obtained.

The length w of the sampling segment is proportional to the vessel radius ($w = k_w R_k$). A correlation process is performed between the sampled profile and a filter which is selected depending on the image type. The maximum of the correlation function is used to determine \mathbf{P}''_{k+d} , second approximation of \mathbf{P}_{k+d} . The vector $\mathbf{P}''_{k+d} - \mathbf{P}_k$ identifies the new vessel direction \mathbf{u}_{k+d} . The brightness $B(x,y)$ is resampled on a segment perpendicular to the direction \mathbf{u}_{k+d} and centred on \mathbf{P}''_{k+d} , so the brightness profile $b'_k(i)$ is obtained. The mean value of the vessel brightness, S_k , is obtained averaging the central elements of the profile $b'_k(i)$, the mean value of the background brightness, N_k , is obtained averaging the outer elements of $b'_k(i)$. The boundary points of the vessel (\mathbf{P}_{b1} and \mathbf{P}_{b2}) are found by comparing the brightness profile $b'_k(i)$ with a threshold related to S_k and B_k (see Figure 2). The middle point of the segment $\mathbf{P}_{b1}\mathbf{P}_{b2}$ is the final estimate of the centerline point, \mathbf{P}_{k+d} , and the length of the segment is the new diameter value, $2R_k$.

In order to track the whole vascular network, the branch points are searched by evaluating the mean value of the brightness (B_m) on a segment positioned at the side of the vessel just tracked and parallel to the vessel direction. If B_m is bigger than an adaptive threshold value, there is a branch. The size of the segment used to evaluate B_m is an empirical parameter based on the trade-off between sensitivity and robustness of the branch detection. Too small a size can lead to the detection of false branch points (false positives), too large a size can prevent the detection of some branches (false negatives).

In the correlation process different filter shapes can be used. The characteristics of two filters were tested: triangular and adaptive filter (obtained by a moving average on the last 3 vessel brightness profiles already sampled). The adaptive filter provides an efficient tracking of a single vessel (in fact it has the best immunity to noise), but it is not selective. It is unable to track a network of vessel: when a branch occurs it is not capable of choosing which vessel to track, causing an early end of the tracking process. Thus, a triangular filter, which is highly selective, was used in this case.

In images without any contrast agent the vessel brightness profile has a different shape if compared to that of vessels in fluoroangiographies: usually it shows a minimum corresponding to the centerline, in this case the brightness profile was inverted before correlation process. Often the profile becomes less regular, because of the reflections which characterise these images. In this case the tracking algorithm was modified. If the brightness profile has two minimum (presence of a reflection) it finds them and fixes the centerline point between these two points.

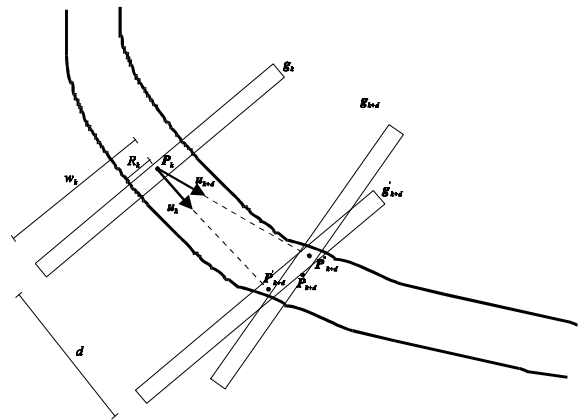


Figure 1: tracking process schema.

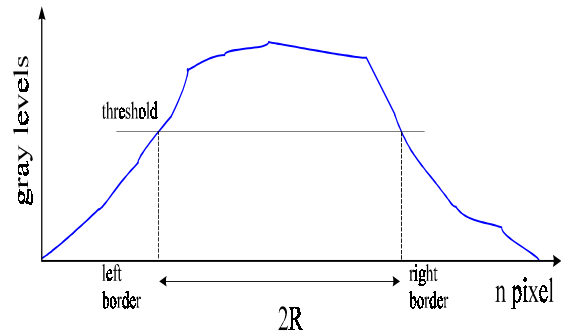


Figure 2: vessel boundary points determination.

3 RESULTS

Simulated images were used to evaluate the performance of the algorithm versus variations of the noise level and vessel characteristics (radius and tortuosity). Two sets of simulated images representing a single vessel, obtained by varying respectively the vessel radius (from 8 to 2 pixel) and the vessel tortuosity (abrupt changes of direction in the angle range 0° - 65°), were generated. The vessel brightness profiles were obtained using Kaiser windows. The synthetic images were corrupted by different gaussian zero mean white noise levels (with SNR from 7 dB up to 34 dB). The signal to noise ratio was evaluated according to the following definition:

$$\text{SNR} = D^2 / \sigma^2$$

where D is the noiseless image contrast while σ^2 is noise variance.

The algorithm proved to be insensitive to the tracked vessel radius and orientation: the mean error on the estimated radius and vessel position remained for the two sets below 1 pixel (the image resolution), even for the lowest SNR level.

To test the capability of the proposed algorithm to detect sudden variations of the vessel radius, a set of simulated images of stenotic vessels was used. The diagram shown in Figure 4 points out that the rms error on the radius of a vessel with a 65% stenosis is below 1 pixel for SNR varying from 7 dB to 34 dB.

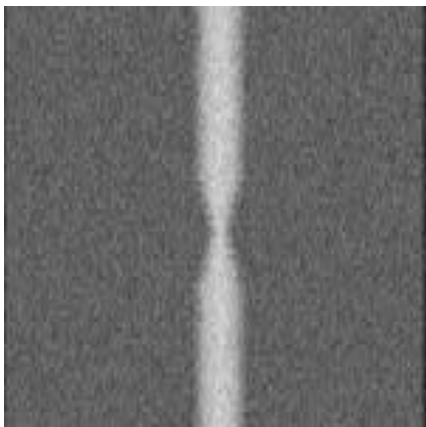


Figure 3: simulated image of stenosis characterised by a 23 dB SNR.

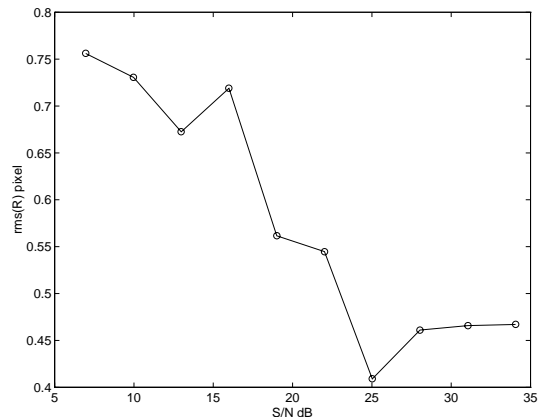


Figure 4: diagram of rms error on the radius versus SNR in a vessel with 65% stenosis.

Finally, the algorithm was tested by comparing the values of radius and position given by the algorithm with the corresponding values obtained by manual contour extractions performed by expert physicians (goldstandard).

In the considered cases a good accordance was found: a mean error of the order of one pixel was obtained for both the position and the radius of the tracked vessels (see the following Tables). Moreover a small number of false negatives and positives was observed in the tracking process.

The algorithm gave results less accurate if applied to images without contrast agent.

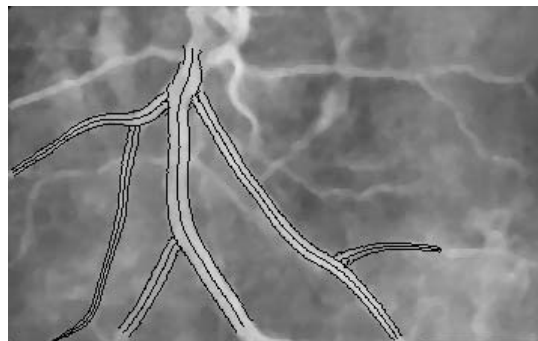


Figure 5: result of the tracking process applied to a fluoroangiography.

branch #	rms	max(r-rI)
1	0.4	1
2	0.5	1

Table I: first column indicates the vessels in Figure 5, r indicates the vessel radius measured by the algorithm, rI is the corresponding goldstandard

<i>branch #</i>	<i>rms</i>	<i>max(P-PI)</i>
1	0.7	2
2	0.8	3

Table II: first column indicates the vessels in Figure 5, P indicates the vessel position measured by the algorithm, PI is the corresponding goldstandard.

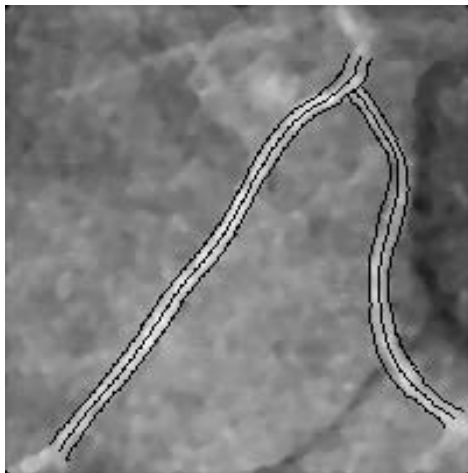


Figure 6: result of the tracking process applied to a fluoroangiography.

<i>branch #</i>	<i>rms</i>	<i>max(r-rI)</i>
1	0.5	3.5
2	0.6	2

Table III: first column indicates the vessels in Figure 6, r indicates the vessel radius measured by the algorithm, rI is the corresponding goldstandard.

<i>branch #</i>	<i>rms</i>	<i>max(P-PI)</i>
1	0.8	4
2	1.2	4

Table IV: first column indicates the vessels in Figure 6, P indicates the vessel position measured by the algorithm, PI is the corresponding goldstandard.

4 CONCLUSIONS

The algorithm proved to be insensitive to the vessel radius and orientation, to be capable of detecting sudden variations of the vessel radius (stenosis), and to give low errors (below 1 pixel) even for very low SNR values (7 dB).

The comparison with goldstandards highlighted that white noise can stop the tracking process and lead to false negatives and that structural noise (uninteresting anatomical structures) can cause false positives.

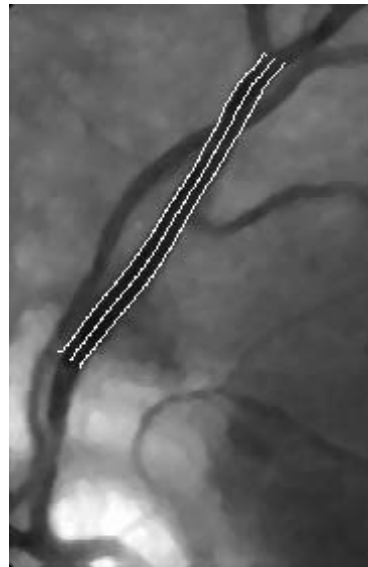


Figure 7: result of the tracking process applied to an image without any contrast agent.

<i>branch #</i>	<i>rms</i>	<i>max(r-rI)</i>
1	0.8	2.5

Table V: first column indicates the vessel in Figure 7, r indicates the vessel radius measured by the algorithm, rI is the corresponding goldstandard.

<i>branch #</i>	<i>rms</i>	<i>max(P-PI)</i>
1	1.2	6

Table VI: first column indicates the vessel in Figure 7, P indicates the vessel position measured by the algorithm, PI is the corresponding goldstandard.

REFERENCES

- [1] S. B. Dimmitt, *et al.*, "Usefulness of ophthalmoscopy in mild to moderate hypertension," *Lancet*, vol. 1, pp. 1103-1106, 1989.
- [2] I. Liu and Y. Sun, "Recursive tracking of vascular networks in angiograms based on the detection-deletion scheme," *IEEE Trans. Med. Imaging*, vol. 12, pp. 334-341, 1993.
- [3] L. Zhou, M. S. Rzeszotarski, L. J. Singerman, and J. M. Chokreff, "The detection and quantification of retinopathy using digital angiograms," *IEEE Trans. Med. Imaging*, vol. 13, pp. 619-626, 1994.
- [4] W. H. Woon, *et al.*, "Confocal imaging of the fundus using a scanning laser ophthalmoscope," *Br. J. Ophthalmol.*, vol. 76, pp. 470-474, 1992.